Human Molecular Genetics, 2014, Vol. 23, No. 20 **5402–5417**
doi:10.1093/hmg/ddu258
Advance Access published on May 22, 2014

STRA6 is critical for cellular vitamin A uptake and homeostasis

Jaume Amengual[1], Ning Zhang[1], Mary Kemerer[1], Tadao Maeda[1,2], Krzysztof Palczewski[1,3,*] and Johannes Von Lintig[1,*]

[1]Department of Pharmacology, School of Medicine, [2]Department of Ophthalmology, School of Medicine and [3]Cleveland Center for Membrane and Structural Biology, Case Western Reserve University, Cleveland, OH 44106, USA

Received April 28, 2014; Revised and Accepted May 19, 2014

Vitamin A must be adequately distributed within the body to maintain the functions of retinoids in the periphery and chromophore production in the eyes. Blood transport of the lipophilic vitamin is mediated by the retinol-binding protein, RBP4. Biochemical evidence suggests that cellular uptake of vitamin A from RBP4 is facilitated by a membrane receptor. This receptor, identified as the *Stimulated by retinoic acid gene 6* (*Stra6*) gene product, is highly expressed in epithelia that constitute blood–tissue barriers. Here we established a *Stra6* knockout mouse model to analyze the metabolic basis of vitamin A homeostasis in peripheral tissues. These mice were viable when bred on diets replete in vitamin A, but evidenced markedly reduced levels of ocular retinoids. Ophthalmic imaging and histology revealed malformations in the choroid and retinal pigmented epithelium, early cone photoreceptor cell death, and reduced lengths of rod outer segments. Similar to the blood–retina barrier in the RPE, vitamin A transport through the blood–cerebrospinal fluid barrier in the brain's choroid plexus was impaired. Notably, treatment with pharmacological doses of vitamin A restored vitamin A transport across these barriers and rescued the vision of *Stra6*$^{-/-}$ mice. Furthermore, under conditions mimicking vitamin A excess and deficiency, our analyses revealed that STRA6-mediated vitamin A uptake is a regulated process mandatory for ocular vitamin A uptake when RBP4 constitutes the only transport mode in vitamin A deficiency. These findings identifying STRA6 as a *bona fide* vitamin A transporter have important implications for disease states associated with impaired blood vitamin A homeostasis.

INTRODUCTION

Microphthalmia is a birth defect with an estimated incidence of 1–3.2 cases per 10 000 live births (1). The association of microphthalmia with extraocular findings is common and can result in complex clinical syndromes (2,3). Among them, the Matthew–Wood syndrome (MWS, also known as Spears Syndrome and Human Micro Ophthalmic Syndrome 9) is characterized by severe bilateral microphthalmia in combination with pulmonary dysplasia, cardiac defects and diaphragmatic hernia (4,5). Additionally brain anomalies, mental retardation and malformations of the kidneys, pancreas and gastrointestinal tract have been described in affected individuals (4–6).

MWS is an autosomal recessive disease associated with mutations in the *stimulated by retinoic acid 6* (*STRA6*) gene (4,5). Both missense and nonsense mutations in this gene have been associated with clinical symptoms of MWS and early childhood death (4,5). However, survivors with *STRA6* null mutations also have been identified in genetic screens of patients with microphthalmia (3,5). Variability in the clinical manifestations of *STRA6* mutations has even been found in consanguine family members. In an Irish family, the same homozygous missense mutation was manifested as either fatal MWS or an isolated microphthalmia (7).

STRA6 encodes an integral membrane protein expressed in embryonic and adult tissues. Epithelia constituting blood–tissue barriers express especially high levels of STRA6, including the retinal pigment epithelium (RPE) of the eyes, ependymal cells of the choroid plexus (CP) in the brain and Sertoli cells of the testis (8). Biochemical studies indicate that STRA6 is the long-proposed cellular receptor for the serum retinol-binding protein, RBP4 (9,10). RBP4, a 21 kDa lipocalin that is produced

*To whom correspondence should be addressed at: Department of Pharmacology (W333), School of Medicine, Case Western Reserve University, 10900 Euclid Avenue, Cleveland, OH 44106, USA. Tel: +1 2163684497; Fax: +1 2163681300; Email: kxp65@case.edu (K.P.); Tel: +1 2163683528; Email: jxv99@case.edu (J.V.L.)

in the liver, transports stored vitamin A to peripheral cells (11,12). Studies in cell culture test systems revealed that STRA6 acts as a retinoid channel that facilitates the bidirectional flux of vitamin A between extracellular and intracellular compartments (9,13–15). In this process, cellular accumulation of vitamin A is driven by esterification via lecithin: retinol acyl transferase (LRAT) (13,14,16).

Birth defects described in MWS patients are consistent with the established role of vitamin A in mammalian development (17,18). Accordingly, studies with recombinant STRA6 demonstrated that disease causing *STRA6* missense mutations either interfered with intracellular STRA6 protein transport or significantly reduced vitamin A uptake (7,19). However, *Stra6* knockout mice display only ocular vitamin A deficiency (20) but otherwise appear healthy (21,22). The phenotype of these mice resembles that of mice deficient for the STRA6 ligand, RBP4; RBP4 knockout mice show ocular retinoid-deficiency and visual impairments (11). Moreover, compound missense mutations in the *RBP4* gene in humans manifest as mild ocular defects and night blindness (23,24).

The discrepancy between the clinical manifestations of mutations in *RBP4* and *STRA6* in humans has led to the speculation that additional genetic alterations must be present in MWS patients (21). Additionally, a role of the STRA6 protein beyond its function as a vitamin A transporter has been proposed but remains controversial (25–27). Furthermore, elevated levels of RBP4 have been associated with diabetes and an increased risk of cardiovascular disease (28,29). Thus, the biochemical role of STRA6 in cellular vitamin A uptake homeostasis from RBP4 and the putative connection between STRA6 and these diseases requires clarification.

The increasing number of cases and their Mendalian inheritance suggest a causative relationship between *STRA6* and MWS (2). We speculated that the variability in the clinical manifestations of *STRA6* mutations is caused by stochastic effects. A putative factor in this process is that dietary vitamin A itself, when present in copious amounts, could mitigate the consequences of STRA6 deficiency. Thus, we generated a *Stra6* knockout mouse model and analyzed the pathological consequences of STRA6 mutations for cellular retinoid uptake by peripheral tissues under variable conditions of dietary vitamin A supply. Our studies both indicate that STRA6 is indeed a *bona fide* vitamin A transporter and provide novel insights into the regulatory mechanism that governs vitamin A homeostasis in peripheral tissues. This information will improve understanding of human disease states associated with impaired blood vitamin A homeostasis and could yield concepts for their prevention and therapy.

RESULTS

Different phenotypic manifestations of mutant *Stra6* alleles

In a classical gene knockout approach, a 603 bp DNA fragment including the start site harboring exon 2 of the *Stra6* gene was replaced by a neomycin resistance selection cassette flanked by two *loxP* sites ($Stra6^{neo}$ allele) (Fig. 1A). Mice homozygous for the mutant *Stra6* allele ($Stra6^{neo/neo}$ mice) were born in a Mendelian ratio, exhibited a very small body size and weight and failed to thrive (Supplementary Material, Fig. S1A). $Stra6^{neo/neo}$ mice had a rounded and enlarged cranium (Supplementary Material, Fig. S1B). This cranial morphology has been described in hydrocephalic mice and magnetic resonance imaging (MRI) confirmed swollen brain ventricles of 21-day-old $Stra6^{neo/neo}$ mice (Supplementary Material, Fig. S2A and B). To analyze the time course of this pathology, we isolated brains from staged mice and performed histology. Coronal cross-sections through the brain revealed that swelling of the ventricles could already be observed in 2-day-old animals (Supplementary Material, Fig. S2C). In 10-day-old $Stra6^{neo/neo}$ mice, swelling had progressed and damage was obvious in some brain areas, e.g. the corpus callosum (Supplementary Material, Fig. S2C). At weaning time (P21), swelling of the ventricular system had progressed and gross damage to the brain area was obvious (Supplementary Material, Fig. S2C).

The CP plays a critical role in controlling intracranial pressure (30). *Stra6* is expressed in ependymal cells of the CP and other parts of the blood–brain barrier (8) and vitamin A has been proposed to play an important role in the development and maintenance of these structures (31). However, $Stra6^{neo/neo}$ mice did not develop other anomalies reported in MWS patients (data not shown). Additionally, published *Stra6* knockout mouse models did not display hydrocephalus and were viable (21). Hence, we wondered if the fatal brain phenotype of $Stra6^{neo/neo}$ mice was related to nonspecific effects of the mutant allele. Several reports indicated that a neo^R selection cassette insertion into a target gene can result in nonspecific phenotypes, e.g. by influencing the expression of neighboring genes (32,33). To address this possibility, we intercrossed mice heterozygous for the $Stra6^{neo}$ allele with a transgenic mouse line that expresses *Cre* Recombinase under control of the adenovirus EIIa promoter. This promoter targets *Cre*-Recombinase activity to early embryonic cells and tissues, including germ cells. We confirmed the *Cre*-Recombinase-mediated excision of neo^R in the progeny of these mice by PCR and DNA sequencing. We then intercrossed these mice to establish mice homozygous for the *Stra6* allele with the 'floxed out' neo^R selection cassette (Fig. 1A). These mice were born in a Mendelian ratio and were viable. Moreover, they developed no apparent signs of hydrocephalus as did their forerunners with the neo^R selection cassette insertion in the *Stra6* gene. To demonstrate that *Stra6* gene function was genetically disrupted in these mice, we isolated mRNA and protein from the RPE. RT-qPCR analysis showed that *Stra6* mRNA expression was highly reduced in these cells (Fig. 1B). For immunoblotting, we tested two commercially available antisera that have been used for STRA6 detection in previous studies (20,25). In our hands, the antibody from Everest Biotech Ltd. (Upper Heyford, UK) did not detect recombinant human STRA6 as previously reported (25). Surprisingly, this antibody detected a protein of 75 kDa in all analyzed tissues including the RPE of the knockout mice (Supplementary Material, Figs S1C and S3A). In contrast, the Abcam (Cambridge, MA, USA) antiserum detected recombinant human STRA6 and a protein of 80 kDa in the RPE of WT mice that was absent in mice homozygous for the mutant *Stra6* allele (Fig. 1C). The same picture emerged when we used Abcam antibody for immunostaining (Fig. 1D). Here, a STRA6 was detected at the basolateral membrane of the RPE in heterozygous mice but was absent in mice homozygous for the *Stra6* mutant allele. Hence, we concluded that STRA6 was genetically disrupted and designated

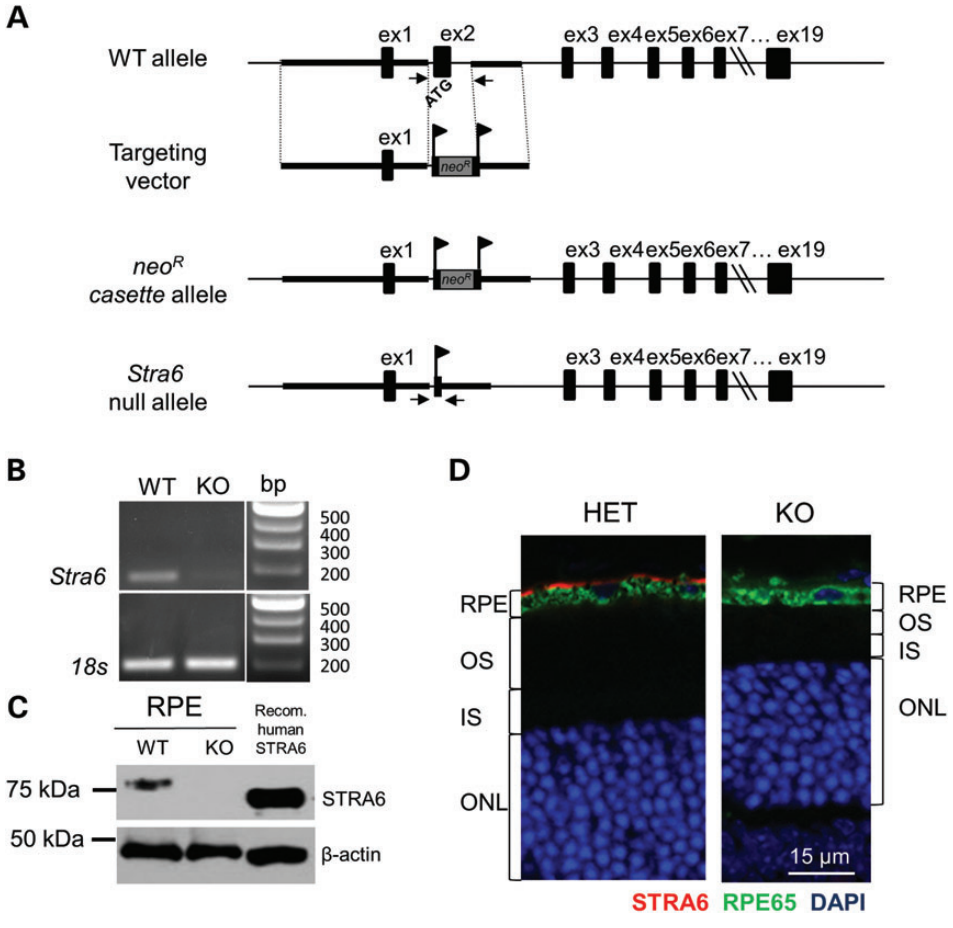

Figure 1. Generation of *Stra6* knockout mice. (**A**) Scheme of the WT and mutant *Stra6* alleles. The targeting vector was designed to replace exon 2 (ex2) with a neomycin cassette (neoR) flanked by two *loxP* sites (indicated by banners). This resulted in the *Stra6* neomycin resistance (neo^R) cassette allele. The neo^R cassette was floxed out by Cre recombinase resulting in the Stra6 null allele. Genotyping of mice was performed by PCR with the primer pair Stra6up/down for the wild-type allele (WT) and Stra6up/KOdown for the null allele (KO) as described in the Materials and Methods. Positions of the primers are indicated by the arrows. (**B**) Total mRNA was isolated from the retinal pigmented epithelium (RPE) of WT and KO mice. RT-PCR for *Stra6* mRNA employing a primer pair that spans exon 3 to exon 5 demonstrates the absence of *Stra6* mRNA in $Stra6^{-/-}$ mice. RT-PCR for 18 s ribosomal RNA was used as loading control. (**C**) Immunoblot of protein extracts isolated from the retinal pigmented epithelium (RPE) of WT and KO mice (20 μg total protein was loaded per lane). Hek293 cells overexpressing human STRA6 were used as a positive control (5 μg total protein) and β-actin was used as a loading control. (**D**) Immunostaining for STRA6 (red) in eye sections of mice heterozygous (HET) and homozygous (KO) for the *Stra6* null allele. Staining for RPE65 (green) was used to visualize the RPE and DAPI (blue) was used to stain the nuclei. ex, exon; OS, outer segments; IS, inner segments; ONL, outer nuclear layer.

these mice as *Stra6* null mice ($Stra6^{-/-}$). These mice and their heterozygous siblings ($Stra6^{+/-}$) were used for further experiments described below.

STRA6 is required for eye development and function

RT-qPCR analysis of murine tissues showed that *Stra6* mRNA expression was highest in the eyes (Fig. 2). Hence, we first analyzed the consequences of STRA6 deficiency in this tissue. HPLC analysis revealed that 4-week-old $Stra6^{-/-}$ mice presented a 7-fold reduction in the amount of total ocular retinoids as compared with their heterozygous siblings (Fig. 3A). This reduction was noted for all visual cycle intermediates, including 11-*cis*-retinal (Fig. 3B). $Stra6^{-/-}$ mice also developed photoreceptor anomalies described for vitamin A-deficient retinas (34). Rod outer segment lengths were shortened and the number of cone photoreceptors was reduced (Fig. 3C). Accordingly, both scotopic and photopic electroretinography (ERG) responses were markedly diminished in the eyes of these mice (Fig. 3D), demonstrating that STRA6 deficiency impaired ocular vitamin A uptake, homeostasis and vision.

We next wondered whether STRA6 is also required for retinoid signaling during ocular development. Thus, we analyzed the morphology of living eyes of 21-day-old mice by optical coherence tomography (OCT) and confocal scanning laser ophthalmoscopy (cSLO). OCT revealed an overall intact lamination of retinal layers in $Stra6^{-/-}$ mice (data not shown). With cSLO, we found pathological alterations at the level of the choroid in the superior area of the eye cup (Fig. 4). Angiography after an indocyanine green (ICG) injection indicated blood vessel leakage into this area (Fig. 4). When compared with wild-type or heterozygous siblings, dissected eye cups of 28-day-old $Stra6^{-/-}$ mice displayed a discolored area in the superior retina (Fig. 5A). Histological sections through this region showed

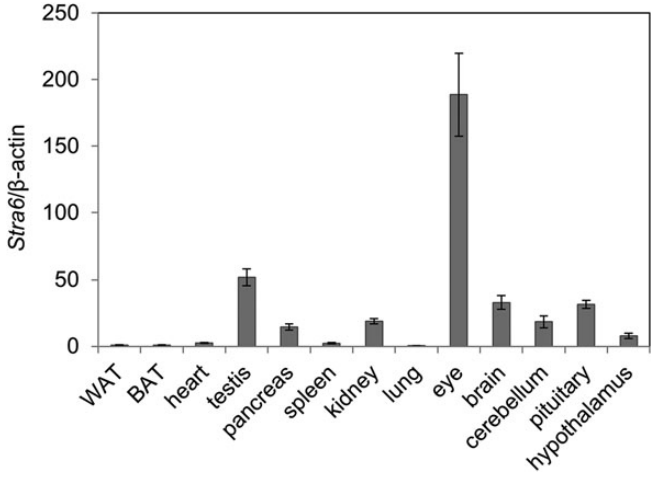

Figure 2. *Stra6* mRNA expression in tissues of 28-day-old mice. Tissues were collected from 21-day-old wild-type mice ($n = 3$). Total RNA was isolated and RT-qPCR analysis for *Stra6* mRNA expression levels was carried out using beta-actin as control. Numbers on the ordinate represent fold changes compared with the expression level in white adipose tissue (WAT) expressed as means ± SEM. BAT, brown adipose tissue.

morphological changes in the RPE and choroid. In the discolored regions, RPE cells manifested large vacuoles and reduced melanin content. The adjacent choroid also was morphologically altered and in some places it was absent (Fig. 5B). Immunohistochemistry analyses for the RPE protein of 65 kDa (RPE65), a key protein of the visual cycle and a specific RPE marker, revealed decreased expression of this isomerase and reduced RPE cell sizes. In some areas, the choroid was thickened and not well connected to the RPE, whereas in others, the RPE was directly joined to the sclera due to complete lack of the choroid (Fig. 5C). In inferior parts of the eyes, this pathology was not evident and the retina, RPE and choroid had a normal lamination (Fig. 5B).

Atrophy of the RPE and choroid also has been reported in patients suffering from *RBP4* missense mutations (24). Therefore, we investigated whether this pathology is characteristic for eyes with impaired vitamin A uptake by analyzing the eyes of $Rbp4^{-/-}$ mice. Similarly, a large discolored area was found in isolated eye cups of $Rbp4^{-/-}$ mice (Supplementary Material, Fig. S4A). In contrast, mice deficient for LRAT that acts downstream of RBP4 and STRA6 in the pathway for chromophore production, did not display this pathology (Supplementary Material, Fig. S4A). An explanation for this finding could be that RBP4 and STRA6 are already required for vitamin A homeostasis of developing eyes, whereas LRAT in conjunction with the retinoid isomerase RPE65 may play a significant role for vitamin A accumulation and chromophore production later in life. Analysis of mRNA expression patterns for *Stra6*, *Lrat* and *Rpe65* confirmed this assumption. Induction of *Lrat* and *Rpe65* mRNA coincided with the developmental time point when visual pigments in photoreceptor are produced around postnatal Day 8 (Supplementary Material, Fig. S4B). *Stra6* mRNA is highly expressed in embryonic stages and, as shown here, throughout all stages of postnatal eye development (Supplementary Material, Fig. S4B).

STRA6 is required for vitamin A transport across the blood–cerebrospinal fluid barrier

Similar to the RPE, ependymal cells of the CP are derived from the ventricular lining of the brain (30). The CP is a specialized structure that synthesizes and maintains cerebrospinal fluid (CSF) to provide nutrients including vitamin A to neurons (30). STRA6 is highly expressed in this structure (Fig. 6A) (8) together with RBP4 and both vitamin A and RBP4 exist in the CSF (35,36). To assess whether $Stra6^{-/-}$ mice show impaired vitamin A transport across the CP, we immunostained their brain sections for RBP4. As it is well established that RBP4 is vitamin A dependently released from hepatocytes, we expected that RBP4 would accumulate in vitamin A deficiency (16). In fact, IHC revealed stronger staining of RBP4 in ependymal cells of the CP in $Stra6^{-/-}$ mice as compared with littermates carrying the wild-type *Stra6* allele (Fig. 6B). Similar results were obtained by immunoblotting with protein homogenates from isolated CP in the fourth ventricle of wild-type and $Stra6^{-/-}$ mice (Fig. 6C). RT-qPCR analysis targeting *Rbp4* mRNA expression in the CP did not reveal significant differences between heterozygous and $Stra6^{-/-}$ mice, thereby eliminating the possibility that a genotypic difference influenced RBP4 expression in the CP (Fig. 6D).

To analyze whether RBP4 accumulation in the CP affects vitamin A homeostasis in the CP and brain, we measured mRNA expression of the RA receptor β (RARβ). RARβ is the main retinoid-binding nuclear receptor of brain cells, including those in the ependyma, and its expression is influenced by retinoid status. RT-qPCR analysis revealed a statistically significant reduction in *Rarβ* mRNA expression levels in the CP and the whole brain of $Stra6^{-/-}$ mice as compared with their wild-type littermates (Fig. 6E).

Pharmacological intervention can restore vitamin A uptake in the eyes and brain

Previously, we had shown that pharmacological doses of retinoids are delivered to the eyes by RBP4/STRA6-independent pathways (37). Here we tested whether a pharmacological dose of vitamin A could bypass the blockage of vitamin A transport across the blood–CSF and blood–retina barriers of $Stra6^{-/-}$ mice. Thus, we treated 2-day-old $Stra6^{-/-}$ mice and littermates with single doses of vitamin A (60 mg/kg) that resulted in highly elevated levels of retinol (ROL) and retinyl esters (RE) in the blood (Fig. 7A and B). Unchanged levels of RBP4 indicated that retinoids were not bound to the vitamin A carrier (Fig. 7C). One day later, we determined RBP4 levels in the CP of sectioned brains of mice. Treated $Stra6^{-/-}$ mice showed significantly reduced staining of RBP4 compared with their vehicle-treated $Stra6^{-/-}$ littermates. Quantification of RBP4 staining in treated $Stra6^{-/-}$ mice revealed that it was comparable to littermates carrying a wild-type *Stra6* allele, indicating RBP4 release into the CSF (Fig. 7D and E).

We next tested whether a pharmacological intervention with retinoids could also bypass the block in vitamin A uptake of STRA6-deficient mouse eyes. To that end, we supplemented 28-day-old $Stra6^{-/-}$ mice ($n = 5$) with a single dose of 0.5 mg vitamin A or vehicle. Two days later, we measured ERG responses of these eyes to different light intensities. These

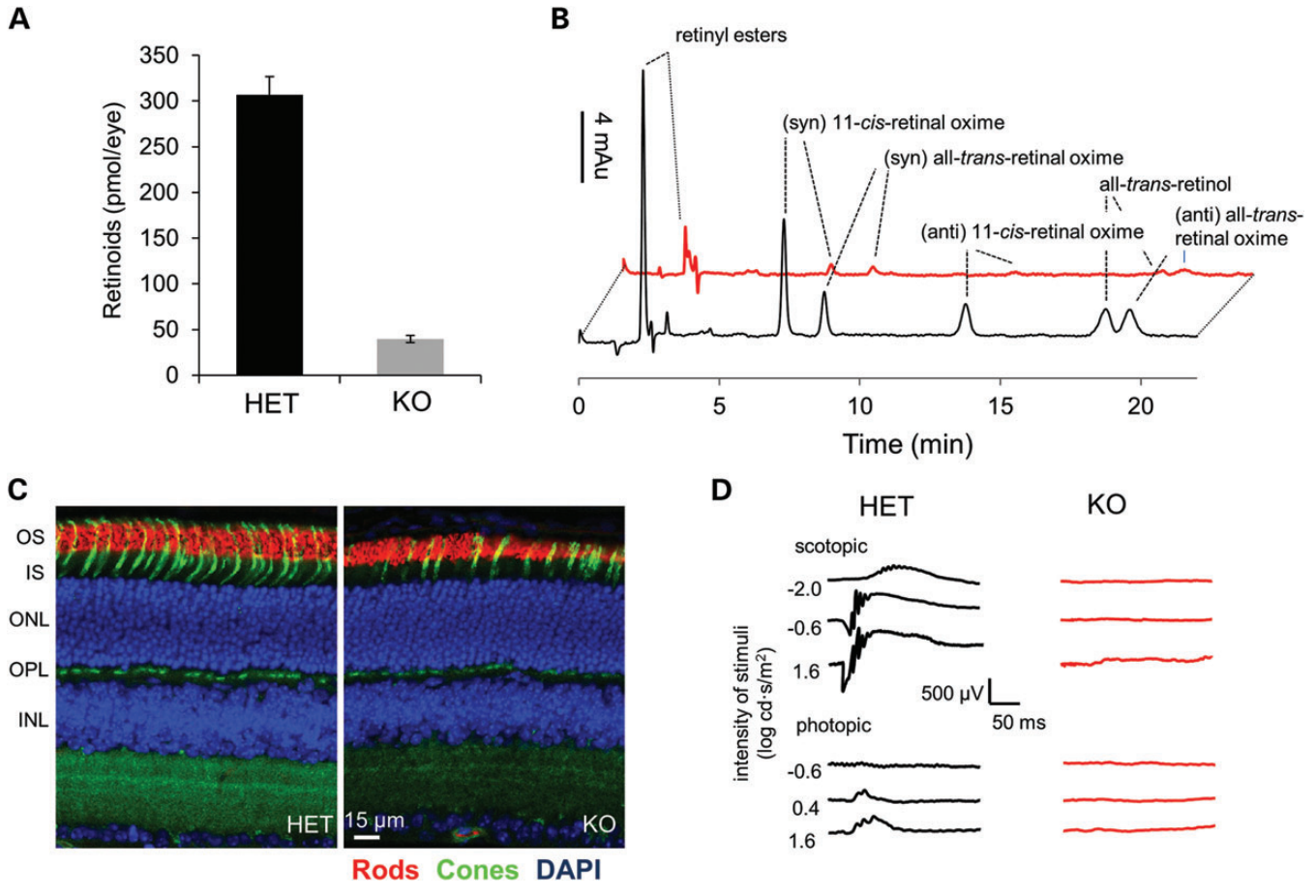

Figure 3. *Stra6*$^{-/-}$ mice evidence blindness and ocular vitamin A deficiency. (**A**) Ocular retinoid content of 21-day-old mice heterozygous (HET) and homozygous (KO) for the *Stra6* null allele. (**B**) HPLC traces (325 nm) of 21-day-old mice heterozygous (black trace) and homozygous (red trace) for the *Stra6* null allele. Identities of individual peaks are indicated in the figure. (**C**) Immunostaining of cone (green) and rod (red) photoreceptors in superior retinas of 21-day-old mice heterozygous (HET) and homozygous (KO) for the *Stra6* null allele. DAPI was used to stain nuclei (blue). Note the reduced thickness of the rod outer segments and inner nuclear layer. (**D**) Scotopic (upper panel) and photopic (lower panel) electroretinograms from 21-day-old mice heterozygous and homozygous for the *Stra6* null allele. OS, outer segment(s); IS, inner segments; ONL, outer nuclear layer; OPL, outer plexiform layer; INL, inner nuclear layer.

analyses demonstrated that this treatment significantly improved scotopic ERG responses of *Stra6*$^{-/-}$ mice (Fig. 8A and B). Interestingly, photopic ERG responses did not improve after this intervention, likely due to the observed early cone photoreceptor cell death in the retina of the *Stra6* knockout mouse model (Fig. 8C). HPLC analysis of ocular retinoids directly confirmed that the ocular retinoid content greatly increased after the intervention with vitamin A (Fig. 8D), demonstrating that a pharmacological dose of this vitamin can enter the eyes by an STRA6-independent uptake mechanism.

Role of STRA6 in vitamin A deficiency

Our mRNA expression profile analyses revealed that most peripheral tissues only express marginal levels of *Stra6* mRNA (Fig. 2). Accordingly, *Stra6*$^{-/-}$ mice were viable and did not display vitamin A deficiency in the blood and/or major storage compartments (Supplementary Material, Fig. S5). This observation confirmed previous studies and indicated that the vitamin A homeostasis of most tissues can be maintained by STRA6-independent pathways when copious amounts of dietary vitamin A are available. Hence, we next tested whether this picture could change when animals were subjected to dietary vitamin A deficiency. We subjected 4-week-old mice to dietary vitamin A restriction and determined retinoid levels at the beginning of the study and again after 6 and 14 weeks of restriction (five mice each). In *Stra6*$^{-/-}$ mice, ocular retinoid content continuously decreased and these compounds were hardly detectable in some mice after 14 weeks of this dietary intervention. In contrast, vitamin A content continuously increased in heterozygous siblings. This finding indicated that stored vitamin A was transported by RBP4 to the eyes and taken up by an STRA6-dependent mechanism in heterozygous mice, whereas this process failed in STRA6-deficient mice (Fig. 9A). To demonstrate this redistribution of vitamin A from storage compartments to the eyes, we determined retinoid levels in the liver and lungs that comprise major storage places for vitamin A in the body. Retinoid levels in these organs decreased with time in both *Stra6*$^{+/-}$ and *Stra6*$^{-/-}$ mice during dietary vitamin A restriction (Supplementary Material, Fig. S6). However, in contrast to the eyes, *Stra6*$^{-/-}$ mice displayed significantly higher levels of stored retinoids as compared with heterozygous siblings. To exclude that differences

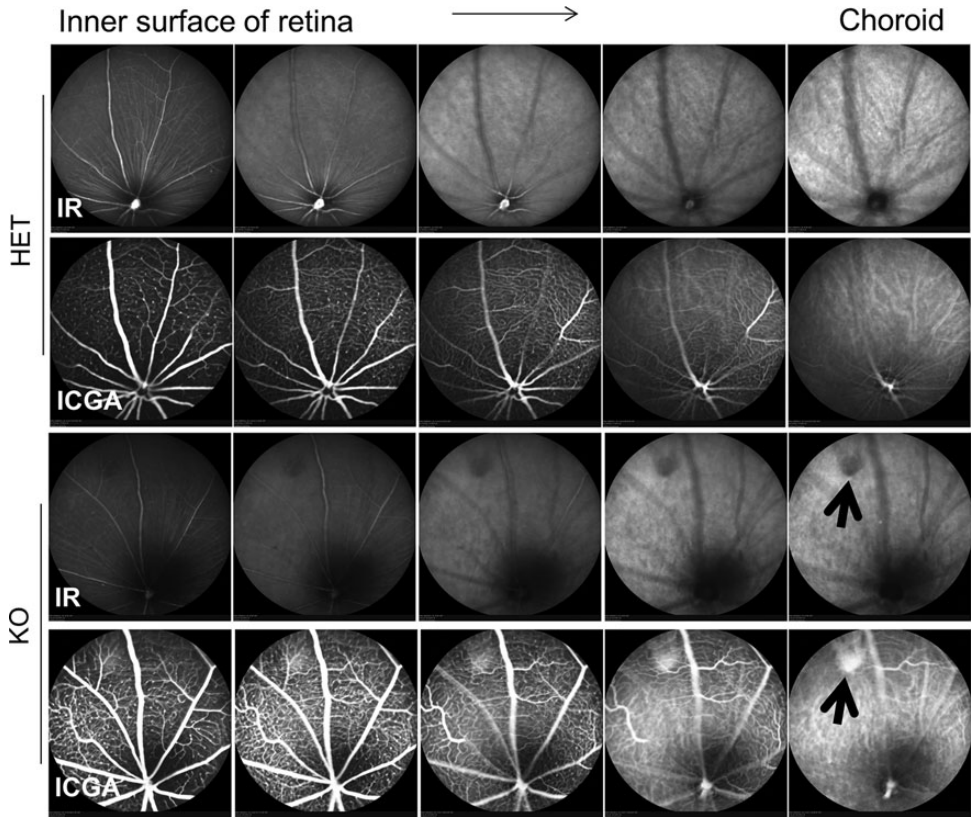

Figure 4. *Stra6*$^{-/-}$ mice display impaired choroidal vascularization. Fundus imaging of 28-day-old mice heterozygous (HET) and homozygous (KO) for the *Stra6* null allele was performed with a cSLO (SpectralisHRA2, Heidelberg Engineering, Heidelberg, Germany) and a 55° lens. The near infrared reflectance image (IR mode, 820 nm laser) was used to align the fundus camera relative to the pupil and thus acquire evenly illuminated fundus images. The ICGA mode (790 nm laser) was used for angiography. After 10 min, mice were injected intraperitoneally with ICG (15 mg/kg, Acros Organics). Arrows indicate the malformed area in the choroid of KO mice.

between genotypes were caused by nonspecific defects, we performed OCT analysis of the eyes of vitamin A deprived mice and analyzed ocular retinoid levels in mice that were kept on a chow diet replete with vitamin A. OCT analyses of the eyes revealed a normal morphology, except for a slightly thinner outer nuclear layer (Fig. 9B), demonstrating that the lack of retinoid uptake did not cause undue morphological changes in STRA6-deficient mouse eyes that might have prevented vitamin A accumulation. Furthermore, HPLC analyses revealed that 18-week-old *Stra6*$^{-/-}$ mice had increased ocular retinoid content when compared with 4-week-old animals, showing that their eyes can acquire dietary vitamin A by an STRA6-independent pathway when copious amounts of this retinoid are present in the diet.

Role of STRA6 in retinoid-induced cellular vitamin A uptake

This study confirmed our previous observation that ocular vitamin A supply is favored in vitamin A deficiency (16). We also had reported that vitamin A uptake from circulating RBP4 can be induced by retinoid signaling in extraocular tissues. In this process, retinoic acid and/or synthetic retinoids can induce *Stra6* and *Lrat* mRNA expression to remove RBP4 bound vitamin A from the circulation and store it in form of retinyl esters in the periphery (16,38). To determine if this process is disrupted in STRA6 deficiency, we treated mice homozygous and heterozygous for the *Stra6* null allele with fenretinide (30 mg/kg) (Fig. 10A). Fenretinide can be metabolized to retinoic acid and induces vitamin A uptake from RBP4 in peripheral tissues as previously demonstrated by a comparative analysis of wild-type and *Lrat*$^{-/-}$ mice (16). RBP4 without bound vitamin A is then rapidly cleared from the circulation by glomerular filtration. As a control, we treated mice with compound A1120 (Fig. 10A). This compound reduces blood RBP4 levels by disrupting the interaction of RBP4 with transthyrethin in an LRAT-independent mechanism (16,39). After treatment with different compounds, we drew blood from the tail veins of mice and measured RBP4 levels by immunoblotting. As expected, this treatment caused a transient decrease of RBP4 serum levels in mice heterozygous for the *Stra6* null allele. In contrast, fenretinide had no such effect in *Stra6*$^{-/-}$ mice as documented by analyses of RBP4 serum levels (Fig. 10B). Treatment with A1120 resulted in a rapid decrease of serum RBP4 levels, thus excluding that the lack of RBP4 clearance from the circulation of fenretinide-treated *Stra6*$^{-/-}$ mice was caused by an indirect effect (Fig. 10C).

DISCUSSION

In the mid-1970s, the first biochemical evidence for a cell surface receptor for RBP4 was noted in the RPE cells of the eyes (40). In the following years, such a receptor also was identified in the CP

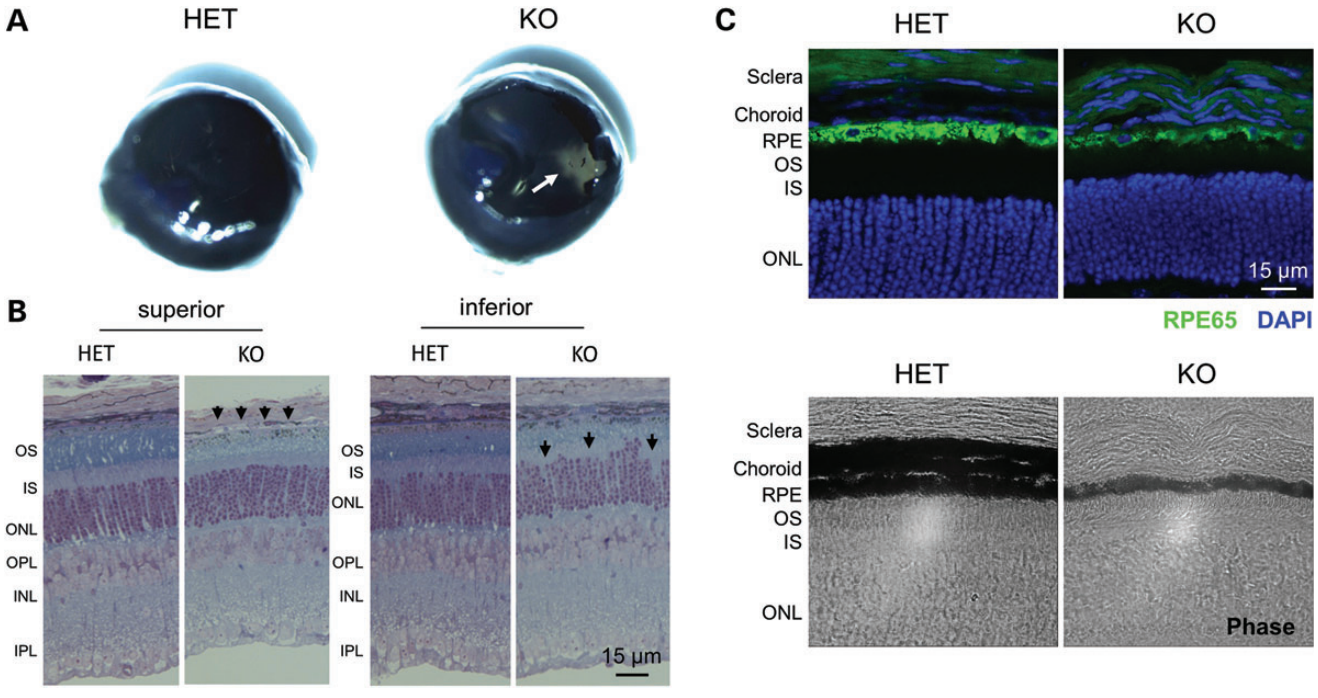

Figure 5. *Stra6*$^{-/-}$ mice develop RPE and choroidal malformations in the superior eye. (**A**) Isolated eye cups of 21-day-old mice heterozygous (HET) and homozygous (KO) for the *Stra6* null allele. White arrow indicates an area of discoloration in KO mice. (**B**) Histological analyses of retinas from 21-day-old heterozygous (HET) and homozygous (KO) for the *Stra6* null allele. KO mice display altered morphology of the RPE, choroid and sclera in superior parts of the retina (arrow heads). In the inferior retina of KO mice, the outer nuclear layer reveals an altered stratification (arrow heads). Note that aside from these malformations, the outer segment layer is significantly reduced in the retina of KO mice. (**C**) (Top panels) Immunostaining for RPE65 (green) of cross-sections of the superior retina of 21-day-old mice HET and KO for the *Stra6* null allele. (Bottom panels) Phase contrast pictures of the same area. Both pictures show a reduction of the RPE and a lack of the choroid in the diseased area of the superior retina. OS, outer segment; IS, inner segment; ONL, outer nuclear layer; OPL, outer plexiform layer; INL, inner nuclear layer; IPL, inner plexiform layer.

of the brain, Sertoli cells of testis and the placenta by radiolabeling assays (for detailed review: 10). Importantly, this receptor not only bound RBP4 but also mediated vitamin A uptake into cells (10,41). In 2007, the molecular identification of an RBP4 receptor was achieved by an elegant strategy that stabilized the fragile RBP4 receptor interaction by protein cross-linking with recombinant-tagged RBP4 and high-affinity purification of the complex (9). The RBP4 receptor turned out to be identical with the multidomain membrane protein STRA6 that previously had been identified as a retinoic acid-inducible protein (42). However, despite emerging biochemical and molecular evidence for receptor-mediated cellular vitamin A uptake, the role of STRA6 in vitamin A biology remains controversial. Here, we provide evidence in a mouse model that STRA6 is a *bona fide* vitamin A transporter critical for vitamin A transport across epithelia that constitute blood–tissue barriers. We further show that the RBP4/STRA6-dependent transport system is subject to regulation by vitamin A and crucial in vitamin A deficiency. Implications of our findings for mammalian vitamin A biology and human disease states associated with mutations in STRA6 are discussed below.

Phenotypes of different *Stra6* alleles

Our classical knockout approach for the generation of mutant mice was based on homologous recombination and insertion of a *neo*^{R} cassette. Mice homozygous for the *Stra6* allele with the *neo*^{R} insertion developed progressive fatal hydrocephalus and died around weaning time. This pathology exhibited full penetrance and was observed in >100 animals homozygous for the *Stra6 neo*^{R} allele but never occurred in heterozygous siblings. We first hypothesized that STRA6 deficiency caused this fatal brain phenotype. This hypothesis was supported by the high expression of *Stra6* in cells that constitute the blood–brain barrier, namely the brain microvasculature and the CP (8). Additionally, brain anomalies such as a thin or absent corpus callosum, arhinencephaly and Dandy–Walker malformation have been reported for MWS patients (4–6). Hydrocephalus has also been described in patients and experimental animal models exposed to excess and deficient levels of vitamin A (43–46) and the vitamin A derivative retinoic acid was recently implicated as a critical embryonic signal for induction of the blood–brain barrier (31). However, the phenotype of our mouse model conflicted with the lack of overt brain pathologies in other STRA6-deficient mouse models (20,22). Thus, we speculated that hydrocephalus could be caused by transcriptional interference of the inserted neomycin cassette with neighboring genes and/or toxicity of the neomycin gene product. Thus, the *neoR* was removed by Cre-recombinase-mediated homologous recombination. In fact, mice homozygous for the floxed *Stra6* null allele were viable and did not show the brain pathology of their forerunners. Interestingly, another *Stra6* knockout mouse line with a deletion of exon 2 exists that shows no brain pathology despite *neoR* insertion (22). The difference between

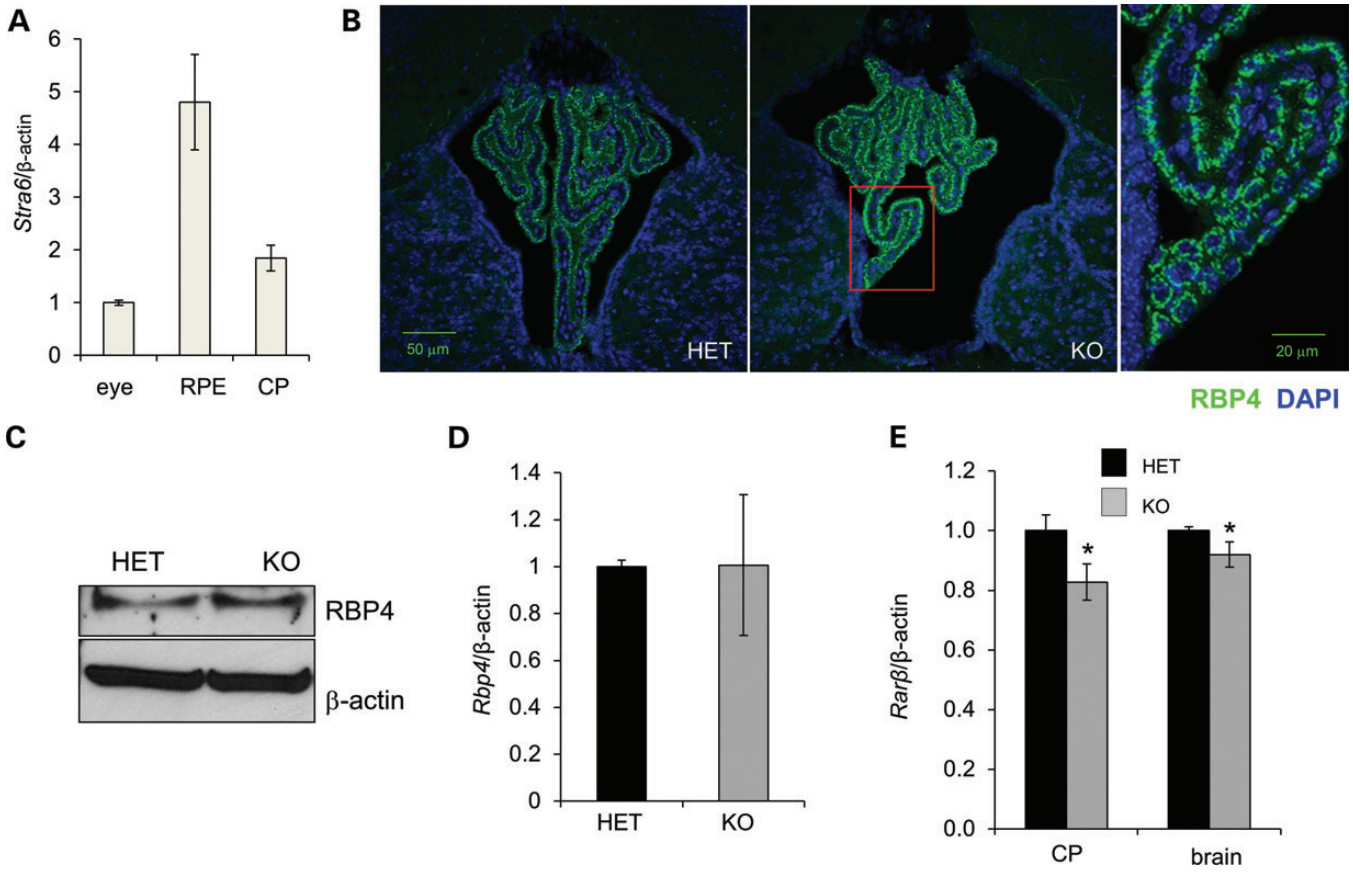

Figure 6. *Stra6*$^{-/-}$ mice accumulate RBP4 in the CP. (**A**) Whole eyes, retina pigmented epithelium (RPE) and CP from the fourth ventricle were collected from 21-day-old wild-type mice ($n = 3$). Total RNA was isolated and RT-qPCR analyses for *Stra6* mRNA expression levels were carried out using β-actin as internal control. Numbers on the ordinate represent fold changes compared with the expression level in whole eye. (**B**) Immunostaining for RBP4 (green) in the CP of 21-day-old *Stra6*$^{+/-}$ (HET) and *Stra6*$^{-/-}$ (KO) mice. In the left most panel, a projected image with a higher magnification for RBP4 staining of RBP4 reveals its localization in ependymal cells of the CP. For all fluorography, DAPI was used to visualize the nuclei (blue). (**C**) Immunoblotting for RBP4 in protein extracts of CP isolated from 21-day-old mice heterozygous (HET) and homozygous (KO) for the *Stra6* null allele. Ten micrograms of total protein per lane were loaded and β-actin was used as a loading control. (**D**) *Rbp4* mRNA levels in isolated CP, and *Rarβ* mRNA levels in CP and whole brain homogenate. β-Actin was used as loading control ($n = 3$ mice/group). Numbers on the ordinate represent fold changes compared with the expression levels in HET animals expressed as means ± SEM.

this and our mouse strain might be explained by the deletion of surrounding DNA. These researchers replaced a 2.7 kbp genomic fragment including exon 2 with a *neo*^{R} cassette, whereas we only replaced a 608 bp genomic region (22). Hence, our observations with different *Stra6* alleles urge the careful evaluation of unexpected phenotypes in knockout mice strains that harbor a *neo*^{R} insertion in the target gene.

Vitamin A transports across the CP and RPE

Radiolabeling studies indicate that the native RBP4 receptor is mainly expressed on epithelia that constitute a blood–tissue barrier such as the RPE and the CP (10,36,40). *Stra6* displays a similar expression pattern as the native receptor (8,9). Our study confirms *in vivo* that STRA6 is critical for vitamin A transport across these barriers. In the brain, ependymal cells of the CP synthesize RBP for the secretion of vitamin A into the CSF (36). In STRA6 deficiency, significantly higher amounts of RBP4 accumulated in the CP than in heterozygous siblings (Fig. 6). Treatment with a pharmacological dose of vitamin A led to a decrease of RBP4 levels in these cells indicative of RBP4's retinoid-dependent release (Fig. 7). Vitamin A deficiency in the CP was corroborated by reduced *Rarβ* mRNA levels in both the CP and the brain (Fig. 6). Similarly, ocular vitamin A uptake was impaired in *Stra6*$^{-/-}$ mice. Consistent with the expression of *Stra6* in the developing embryonic and postnatal eyes (8) (Supplementary Material, Fig. S4), *Stra6*$^{-/-}$ mice displayed ocular malformations (Figs 4 and 5). In a large area of the superior eye cup, the choroid was not properly formed and the RPE was directly adjacent to the sclera of the eyes. Notably, we found a similar pathology in the eye cup of *Rbp4*$^{-/-}$ mice, suggesting that lack of RBP4 and STRA6 has comparable pathological consequences for the murine eye (Supplementary Material, Fig. S4). Since high-dose vitamin A supplementation did not improve these anomalies in *Stra6*$^{-/-}$ mice (data not shown), they likely are due to a lack of vitamin A uptake and production of RA during eye development. Evidence for developmental RA deficiency of the eyes previously has been obtained in STRA6-deficient mice (21). In line with this observation, the malformations in the choroid of STRA6-deficient mice are consistent with the known role of RA in the patterning of periocular mesenchymal tissue (47). Additionally, evidence from RPE cell cultures

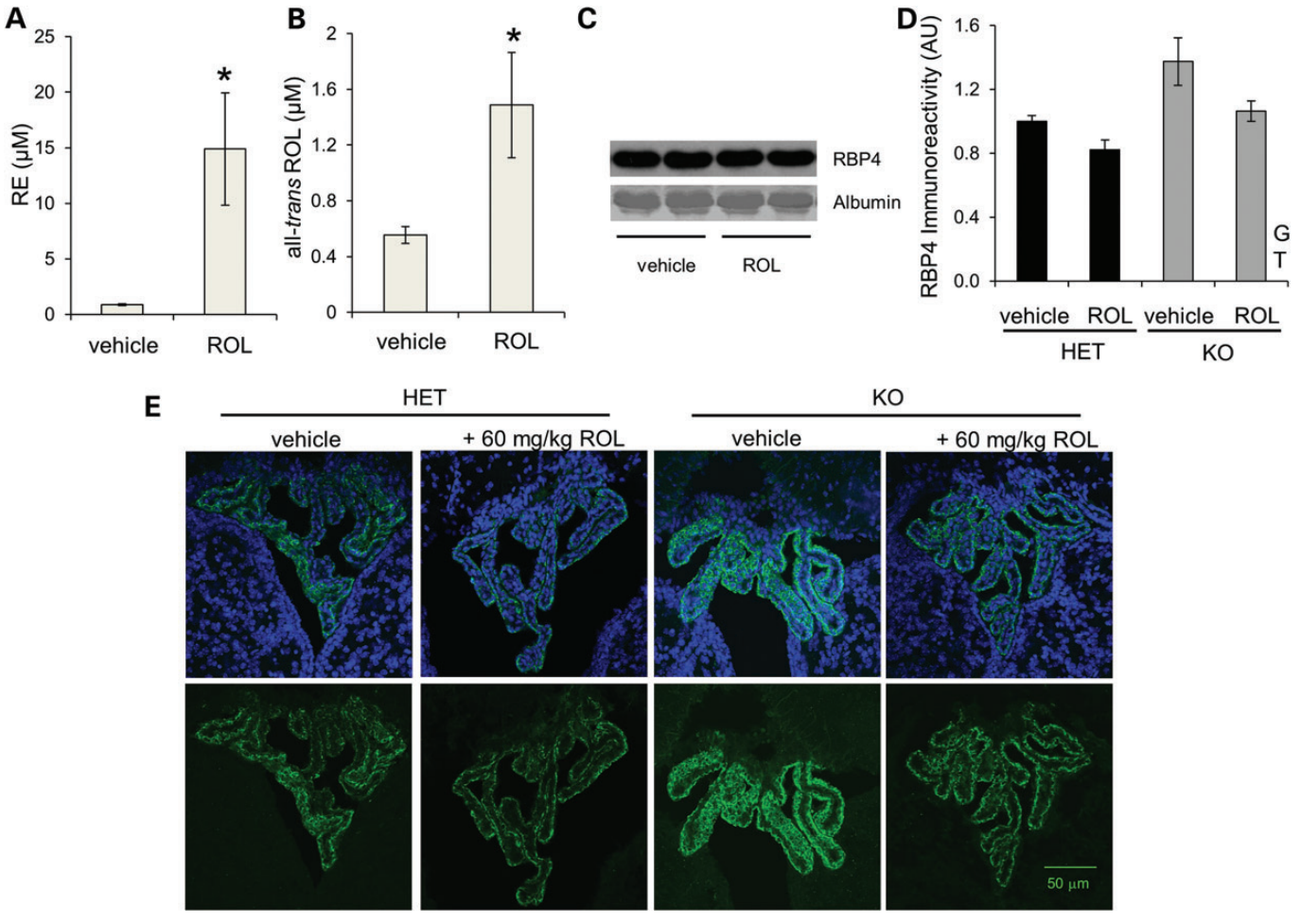

Figure 7. Pharmacological doses of vitamin A promote RBP release in the CP. Two-day-old mice heterozygous (HET) or homozygous (KO) for the *Stra6* null allele were orally supplemented with 60 mg/kg of body weight of ROL dissolved in canola oil or vehicle only as a control. Mice were sacrificed 4 h later for blood and brain collection. (**A**) Circulating retinyl esters (RE), (**B**) free ROL and (**C**) immunoblotting of RBP4 levels in the serum of vitamin A or vehicle-treated mice upon euthanasia. (**D**) RBP4 immune-reactivity was quantified in the CP 1 day post-vitamin A treatment. (**E**) Representative immunostaining for RBP4 (green) in the CP of mice. DAPI was used to visualize the nuclei (blue). Numerical data represent the means ± SEM. *, $P<0.05$; Student's *t*-test. G, genotype effect in two-way ANOVA analysis ($P < 0.05$); T, effect of the ROL treatment in two-way ANOVA analysis ($P < 0.05$). AU; arbitrary units.

suggests an important role of RA in the regulation of RPE differentiation (48), proliferation (49), melanogenesis (50), barrier function (51) and angiogenesis gene expression (52,53). In another *Stra6* knockout mouse model, a persistent primary vitreous body has been described (20). We did not observe this pathology in our $Stra6^{-/-}$ mice, whereas the described malformations of the RPE and choroid had complete penetrance in all animals. Notably, the primary vitreous body is a transient structure consisting of fibroblastic cells stemming from the periocular mesenchyme and a capillary network given off by the hyaloid artery (20). Hence, this pathology may result from a patterning defect of the periocular mesenchyme as well. In the retina, $Stra6^{-/-}$ mice displayed shortened rod outer segments and a highly reduced number of cones. These photoreceptor cell anomalies have previously been reported in other mouse models that display chromophore deficiency (Fig. 9) (54–57). Together, our analyses indicated that STRA6 plays a role both for eye development and subsequent function and maintenance of photoreceptors.

STRA6 and vitamin A homeostasis

Our studies confirmed a previous observation that ocular vitamin A uptake was not completely abrogated in STRA6 deficiency (Fig. 3) (20). Ocular retinoid content of $Stra6^{-/-}$ mice even increased during adolescence when mice were kept on a high vitamin A diet (Fig. 9), a phenomenon previously described in RBP4-deficient mice (11). Similar to $Rbp4^{-/-}$ mice, most other peripheral tissues did not display altered retinoid levels in STRA6 deficiency (Supplementary Material, Fig. S5) (21,22). A minor role of STRA6 in vitamin A uptake of peripheral tissue is consistent with the very low expression levels of *Stra6* mRNA in most peripheral tissues (Fig. 2). These observations clearly indicate that vitamin A can be delivered to peripheral tissues by mechanisms that do not involve the retinoid channel and this process likely depends on dietary vitamin A from chylomicrons. Accordingly, the picture changed when we subjected mice to dietary vitamin A restriction during adolescence. In $Stra6^{-/-}$ mice, ocular vitamin A content continuously

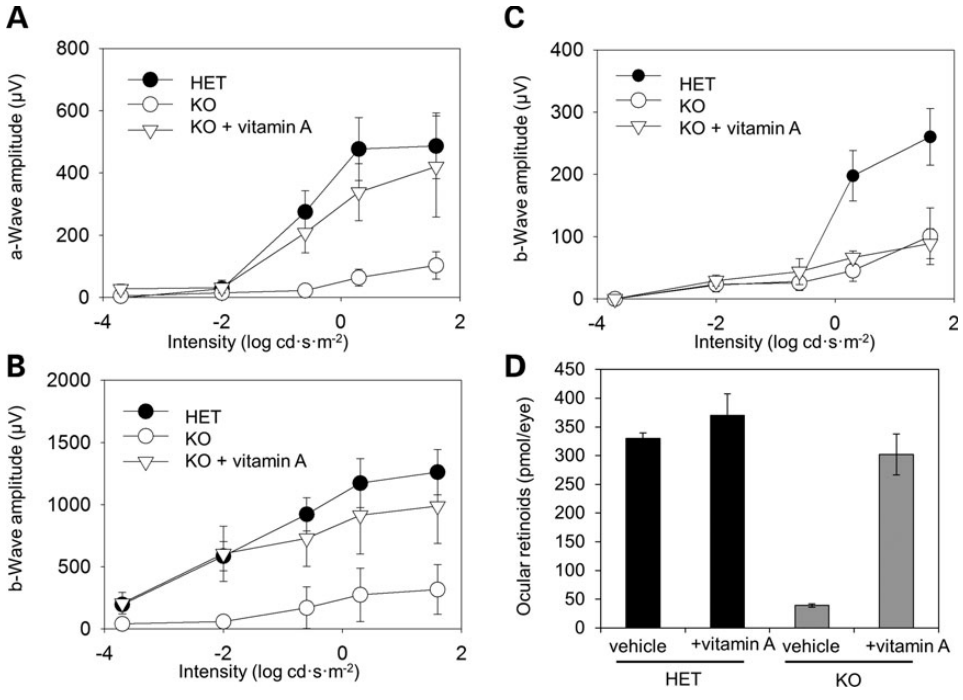

Figure 8. Pharmacological doses of vitamin A restore vision in *Stra6*$^{-/-}$ mice. Scotopic (**A** and **B**) and photopic (**C**) single flash ERG analyses of 28-day-old mice heterozygous (HET) or homozygous (KO) for the *Stra6* null allele. KO mice were raised on a standard chow diet and either gavaged or not with 0.5 mg all-*trans*-retinol per animal (+ VitA). Values are expressed as means ± SEM ($n = 3$ per genotype and dietary condition). (**D**) Total ocular retinoid contents of mice were determined by HPLC analysis and expressed as means ± SEM ($n = 3$ per genotype and dietary condition).

decreased under this restriction and was below detection level of the HPLC system in some animals after 14 weeks of deprivation. In contrast, ocular vitamin A content increased in mice carrying a wild-type *Stra6* allele. This finding demonstrated that STRA6 is mandatory for ocular retinoid vitamin A uptake from circulating RBP4 that constitutes the major transport mode for vitamin A during its dietary deficiency. The increase in ocular vitamin A in mice carrying a wild-type *Stra6* allele under dietary vitamin A deprivation was mirrored by a decrease in hepatic retinoid levels, indicative of a redistribution of this vitamin from its storage compartments to the end organ. Accordingly, *Stra6*$^{-/-}$ mice showed increased hepatic vitamin A levels as compared with their heterozygous siblings because vitamin A transport was impaired.

We have previously shown that retinoid uptake of the eyes is favored over other peripheral tissues under dietary vitamin A restriction (16). This phenomenon is explained by a vitamin A-dependent regulation of this process in extraocular peripheral tissues that is correlated with transcriptional upregulation of both *Stra*6 and *Lrat* gene expression (16). Direct involvement of STRA6 in this process was evidenced by our experiments with fenretinide (Fig. 10). Treatment with this synthetic retinoid led to a rapid decrease in serum RBP4 levels in mice carrying a wild-type *Stra6* allele but not in *Stra6*$^{-/-}$ mice. This finding implicates retinoid signaling in the regulation of vitamin A uptake homeostasis in extraocular peripheral tissues. In obese mouse models, *Stra6* expression is highly decreased in adipocytes and serum RBP4 levels are increased (26). Notably, fenretinide treatment induces retinoid signaling and improves insulin resistance in mice (58). Hence, the role of STRA6 in regulating blood vitamin A homeostasis, including RBP4 levels, warrants further investigation.

In vitamin A deficiency, pulmonary retinoid levels continuously decreased in both *Stra6*$^{+/-}$ and *Stra6*$^{-/-}$ mice during dietary vitamin A restriction (Supplementary Material, Fig. S6). This decrease was at least partially caused by the consumption of stored vitamin A for the production of biologically active vitamin A derivatives that play important roles for the functioning of this tissue. Notably, *Stra6*$^{-/-}$ mice displayed significantly higher pulmonary levels of vitamin A as compared with their heterozygous siblings. The increased pulmonary retinoid levels of *Stra6*$^{-/-}$ mice during dietary vitamin A restriction might be explained by two different scenarios. First, the lack of ocular vitamin A uptake from RBP4 in STRA6 deficiency results in delivery of the cargo to the lungs. Pulmonary uptake then involves either the recently proposed RBP4 receptor 2 (59) or is mediated by passive diffusion (21). Second, the increased pulmonary retinoid levels reflect the ability of STRA6 to transport vitamin A in both directions (13). Thus, in dietary vitamin A deficiency, pulmonary vitamin A is delivered to the circulation to replenish unbound RBP4 with cargo. Such a role for STRA6 in leveling tissue vitamin A has recently been elegantly demonstrated for adipocytes (27). In STRA6 deficiency, this process would be abrogated, thus explaining the increased pulmonary vitamin A levels in knockout mice.

Implications for MWS

Our analyses revealed that STRA6 plays a pivotal role in the development and functioning of murine eyes. In humans, both nonsense and missense mutations in *STRA6* have been

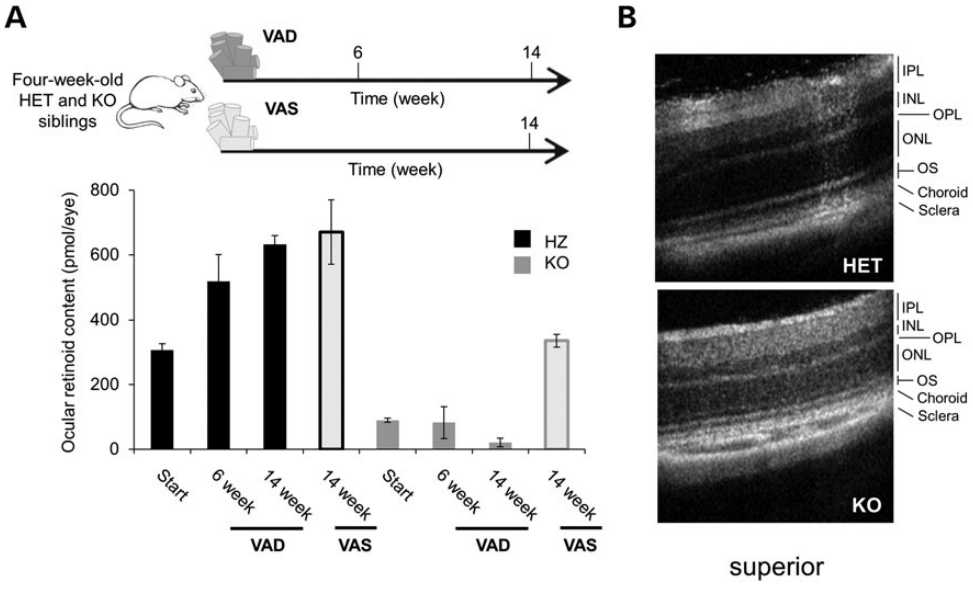

Figure 9. STRA6 is critical for photoreceptor maintenance under dietary vitamin A restriction. (**A**) Scheme of the dietary intervention. Mice heterozygous (HET) and homozygous (KO) for the *Stra6* null allele were raised on vitamin A rich chow. At weaning time mice were subjected to dietary vitamin A restriction. As a control, mice were continuously kept on vitamin A-rich chow. (**B**) Ocular retinoid content in mice of different genotypes and dietary groups. (**C**) SLO analysis of mice subjected to dietary vitamin A restriction. Note that the outer segment layer is greatly reduced in KO mice.

associated with severe bilateral microphthalmia. This more severe manifestation of ocular malformations in STRA6 deficiency might be explained by differences in vitamin A biology between murine and human eyes. This assumption is corroborated by recent genetic evidence showing that mutations in the gene encoding the retinoic acid producing enzyme *ALDH1a3* cause a similar eye phenotype in humans (60), whereas *Aldh1a3* knockout mice display no microphthalmia (47,61). Additionally, the extrauterine eye development and delivery of dietary vitamin A via breast milk may make murine eyes less dependent on STRA6.

In humans, mutations in *STRA6* are associated with birth defects ranging from isolated micropthalmia to the full spectrum of MWS with cardiac and pulmonary syndromes. In this respect, we propose that variability in maternal vitamin A status and delivery to the fetus may at least partially account for the variability of the STRA6 phenotype. Studies in mice demonstrate that both dietary and stored vitamin A can be transported through the fetal–maternal–blood barrier. Dietary vitamin A in chylomicrons is delivered to the embryo by a lipoprotein lipase-mediated mechanism (62). Vitamin A from hepatic stores is delivered to the embryo through an RBP4-dependent transport process and such transport plays a critical role in dietary vitamin A deficiency (63). Notably, dietary vitamin A restriction of $Rbp4^{-/-}$ mice leads to malformations in the offspring that resemble the birth defects described in MWS patients (63). Biochemical evidence has been provided that an RBP4 receptor is expressed in the placenta that mediates vitamin A transport (64,65). In mice, it is yet not clear whether this receptor is STRA6 or the recently identified RBP4 receptor 2 that are both expressed in this tissue (59,66). Thus, variation of dietary vitamin A supply during critical periods of pregnancy could be an important modulator of MWS severity treatable by pharmacological doses of vitamin A. $Stra6^{-/-}$ mice will be a versatile future animal model to study this and other unresolved questions related to vitamin A homeostasis and its relationship to disease.

MATERIALS AND METHODS

Generation of *Stra6* knockout mice

By a classical knockout approach, mice with a mutant *Stra6* allele were generated by the *inGenious* Targeting Laboratory (Stony Brook, NY, USA). Briefly, through homologous recombination in embryonic stem cells, a 603 bp DNA fragment including exon 2 of the murine *Stra6* gene (containing the translational start site) was replaced by a neomycin resistance expression cassette (neo^R) flanked by two *loxP* sites. The targeting strategy is illustrated in Figure 1A. After selection with G418 antibiotic, surviving clones were expanded for PCR analysis to identify recombinant embryonic stem cells. Homologous recombination was confirmed by Southern blotting and PCR and the resulting preparation was microinjected into C57BL/6 blastocysts. Chimeric mice were generated and screened for germ line transmission. Chimeric males were backcrossed with female C57BL/6 mice to produce offspring heterozygous for the *Stra6 neomycin* allele ($Stra6^{neo}$). Heterozygous mice carrying the $Stra6^{neo}$ allele then were crossed with B6.FVB-Tg(EIIa-cre)C5379Lmgd/J mice (Jackson Laboratories, Bar Harbor, ME, USA) to excise the neomycin cassette by Cre-recombinase-mediated recombination. The EIIa promoter targets expression of Cre-recombinase to very early embryonic stages. Thus, neo^R is lacking in a wide range of tissues including germ cells. In the offspring, we confirmed removal of neo^R by PCR and DNA sequencing and designated the resulting allele as a *Stra6* null allele (Fig. 1A). Mice heterozygous for the Stra6 null allele were intercrossed to establish $Stra6^{-/-}$ mice.

Genotyping for recombinant Stra6 alleles

Genomic DNA was isolated and purified from mouse tail biopsies. Genotyping was carried out with a combination of different PCRs (Fig. 1). PCRs were performed with the following primers:

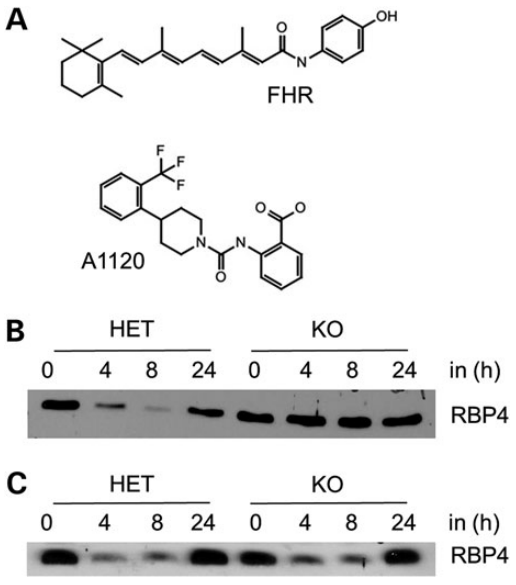

Figure 10. Fenretinide (FHR) but not A1220 decreases RBP and retinol serum levels in a STRA6-dependent manner. (**A**) Molecular structure of the two RBP-lowering agents used, namely the synthetic retinoid fenretinide (FHR) and A1120. (**B** and **C**) Serum RBP4 levels in mice heterozygous and homozygous for the *Stra6* null allele after a single gavage with (B) 30 mg FHR/kg) and (C) 30 mg A1120/kg. Blood samples from the tail vein of each animal were collected ($n = 3$ per genotype and condition) at time points shown. Representative immunoblots for serum RBP4 are displayed.

stra6up 5′-CCA GCA AGA GCC TGA ACC-3′; Stra6down 5′-TCT TCT TCC TTG ACC CCA GA-3′ (for the wild-type allele); Stra6up and Stra6KOdown 5′-CGT ACG CCG GCT TAA GTG TA-3′ (for the KO allele). SYBR reagents (Applied Biosystems, Carlsbad, CA, USA) with commercially available primers (Integrated DNA Technologies, Coralville, IA, USA) were used to detect the presence of the *Cre* transgene, and the floxed out *Stra6* null gene was genotyped with Stra6up (see above) and Stra6KO2down 5′- (5′-CGT ACG CCG GCT TAA GTG TA-3′). The absence of *Stra6* mRNA expression was confirmed with a primer set designed to amplify part of exon 3, all of exon 4 and part of exon 5. mRNA obtained from the RPE was isolated and retro-transcribed into cDNA (see below for details). Primers used for this purpose were; Stra6_mRNAup 5′-TCA CTG TCG TTC CTG GTT CT-3′; Stra6_mRNAdown 5′-GGC ATA GGT TGC TGA AGA GG-3′. To further validate the absence of STRA6 in our knockout mouse model, we conducted dot blot, immunoblotting and IHC analyses with a commercially available antibody directed against the C-terminus of human STRA6 (Abcam) and murine STRA6 (EB07811) (Everest Biotech Ltd.); see below for more details. Hek293 cells overexpressing human STRA6 were used as a positive control in immunoblotting (13).

Animals, husbandry and diets

Mice were maintained on either a regular chow diet (Prolab RMH 3000, vitamin A content 29 000 IU/kg diet) or a vitamin A-deficient diet based on the AIN-93 (Research Diets, Inc. New Brunswick, NJ, USA). Mice were kept with *ad libitum* access to food and water at 24°C in a 12:12 h light–dark cycle. All animal procedures and experiments were approved by the Case Western Reserve University Animal Care Committee and conformed to recommendations of both the American Veterinary Medical Association Panel on Euthanasia and the ARVO Statement for the Use of Animals in Ophthalmic and Vision Research.

Assay for RPB4 release from the CP

Two-day-old mice were given a single oral dose containing ROL (60 mg/kg body weight) dissolved in canola oil. Mice were anesthetized 24 h after treatment by intraperitoneal injection with 20 μl/g body weight of an anesthetic cocktail containing ketamine (80 mg/kg bw) and xylazine (20 mg/kg bw) diluted with 10 mM sodium phosphate (pH 7.2) and 100 mM NaCl. Blood then was collected for serum isolation and the brain was removed and immediately fixed for immunostaining analyses (see below).

Rescue of vision

Twenty-eight day old mice (n = 3) were gavaged with 0.5 mg ROL in canola oil. Mice were anesthetized 24 h after the last treatment by a 20 μl/g bw intraperitoneal injection of an anesthetic cocktail containing ketamine and xylene (see above) and ERG measurements were performed (see below for details). Immediately afterwards, mice were euthanized prior to ocular retinoid quantification and histological analyses.

Electroretinography

All ERG procedures were performed using published methods (67). Briefly, mice under a safety light were anesthetized by intraperitoneal injection of a ketamine/xylene anesthetic cocktail (see above for composition) and their pupils were dilated with 1% tropicamide. A contact lens electrode was placed on the eye and a reference electrode and ground electrode were positioned on the ear and tail, respectively. Both scotopic and photopic ERGs were recorded with a computerized system (UTAS E-3000; LKC Technologies, Inc., Gaithersburg, MD, USA).

HPLC analyses of retinoids

Retinoids were extracted from 100 μl of serum, one whole eyecup or a tissue homogenate in PBS containing 100 mg of tissue. All retinoid isolation procedures took place under a dim red safety light (600 nm). Hydroxylamine (200 μl, 2 M) was added to the eyecup before the tissue was homogenized. Retinoid extraction was performed twice with a mixture containing 200 μl of methanol, 400 μl of acetone and 500 μl of hexane. HPLC analysis was performed on a normal-phase Zorbax Sil (5 μm, 4.6 × 150 mm) column (Agilent, Santa Clara, CA, USA). Chromatographic separation was achieved by isocratic flow of 10% ethyl acetate/90% hexane at a flow rate of 1.4 ml/min. For quantification of molar amounts of retinoids, the HPLC was previously scaled with synthesized standard compounds.

Immunoblotting

All tissue samples were homogenized in M-PER mammalian protein extraction reagent (Thermo Scientific, Marietta, OH, USA) following the manufacturer's instructions. For STRA6 detection, a rabbit polyclonal antibody (Abcam) and a goat Anti-STRA6 antibody (EB07811) (Everest Biotech Ltd.) were tested at a 1:500 dilution. RBP4 serum levels were determined as previously described (68) with a rabbit anti-human RBP4 serum (Dako-Cytomation, Denmark). Tissue and cell lysates were dissolved in SDS–PAGE-loading buffer (6% SDS, 15% β-mercaptoethanol, 20% glycerol, 0.005% bromophenol blue in 0.125 M Tris, pH 8) and boiled for 5 min. For STRA6 immunodetection, samples were never boiled but directly loaded to avoid protein aggregation prior to SDS–PAGE. After proteins were resolved by SDS–PAGE, they were electroblotted onto PVDF membranes (Bio-Rad, Hercules, CA, USA). Membranes then were blocked with fat-free milk powder (5%, w/v) dissolved in Tris-buffered saline (15 mM NaCl and 10 mM Tris–HCl, pH 7.5) containing 0.01% Tween-100 (TBS-T), washed and incubated overnight at 4°C with an appropriate primary antibody. β-Actin antiserum (Cell Signaling, Boston, MA, USA) at a dilution of 1:1000 served as a loading control for total protein-level determinations. The secondary antibody employed was horseradish peroxidase-conjugated anti-rabbit IgG (Promega, Madison, WI, USA) at a dilution of 1:5 000. Immunoblots were developed with the ECL system (GE Healthcare, Cleveland, OH, USA). Quantification of scanned immunoblot bands was performed with ImageJ software.

Total RNA isolation and RT-qPCR analyses

Total mRNA isolation was carried out with TRIzol reagent (Invitrogen, Carlsbad, CA, USA) according to manufacturer's instructions. RNA concentration and purity was measured with a Nano-drop spectrophotometer (ND-1000, Thermo Scientific). The Applied BioSystems retrotranscription kit (Applied BioSystems) was used to reverse transcribe 0.5 μg of total RNA to cDNA. RT-qPCR was carried out with TaqMan probes (Applied BioSystems) for STRA6 (Mm00486457_m1) and RBP (Mm00803266_m1). A β-actin (Mm01205647_g1) probe set was used as an endogenous control. All real-time experiments were done with an ABI Step-One Plus RT-qPCR instrument (Applied BioSystems).

Treatment with RBP-lowering agents: blood and tissue collection

At 8 a.m., a small blood sample was collected from the tail vein of each mouse to determine the RBP level at time point ($t = 0$) and kept on ice until serum separation. Immediately thereafter, animals were gavaged with 30 mg/kg body weight of either fenretinide (Toronto Research Chemicals, Canada) or A1120 (Sigma, St. Louis, MO, USA) dissolved in 200 μl canola oil with the same volume of canola oil used as a vehicle control. Tail vein blood samples were collected at 4, 8 and 24 h after treatment. To determine RBP4 serum levels, 2 μl of serum was diluted with 40 μl of PBS containing complete Mini EDTA-free protease inhibitor (Roche Diagnostics, Indianapolis, IN, USA), and 4 μl of this solution was used for immunoblot analysis. SDS–PAGE and immunoblotting were performed as described above.

Histological staining and analysis of brain sections

For histological and immunohistochemical analysis of central nervous system tissues, mice under anesthesia provided by a mixture containing ketamine (80 mg/kg bw) and xylazine (20 mg/kg bw) in 10 mM sodium phosphate, pH 7.2, with 100 mM NaCl were perfused with 4% paraformaldehyde solution in PBS. Thirty-micrometer-thick coronal sections of the brain were cut on a Leica cryostat CM1850 (Leica Microsystems, Buffalo Grove, IL, USA). Nissl staining was performed for global brain visualization.

Three to six free-floating sections from each mouse were used (4–6 animals per genotype) for IHC analyses. Sections were blocked and permeabilized for 1 h in blocking buffer (phosphate saline buffer and triton 0.1%, with 5% goat serum (Sigma) and 1% bovine serum albumin (Sigma) and then incubated overnight at 4°C with primary rabbit polyclonal anti-RBP (DakoCytomation) antibody at a 1:400 dilution in blocking buffer. Following incubation, RBP4 was treated with anti-rabbit conjugated Alexa 488 secondary antibody (Invitrogen) at 1:400 dilution in blocking buffer and counterstained with DAPI nuclear stain.

Histology and immunohistochemistry of eye sections

For histology, mouse eye cups were first fixed overnight by immersion in 5% glutaraldehyde/4% paraformaldehyde, pH 7.4, at 4°C. Then they were washed with 0.13 M sodium phosphate, pH 7.3, and secondarily fixed with 1% OsO_4 in 0.1 M sodium phosphate, pH 7.4, for 2 h at room temperature. Eye cups subsequently were dehydrated through an ethanol series (50, 70, 80, 90, 95 and 100%), transitioned to epoxy embedding medium with propylene oxide, and embedded for sectioning in Eponate 812. Sections for morphological study were cut at 1 μm with a microtome (Leica RM2255) and stained with toluidine blue. Digital images were captured with a Leica CRT 6000 microscope.

For immunohistochemistry, mouse eye cups were fixed with 4% paraformaldehyde in 0.1 M sodium phosphate buffer (pH 7.4) for 2 h. Fixed tissues were dehydrated with 30% sucrose in PBS, embedded in Optimal Cutting Temperature compound sucrose mixture (1:1 Optimal Cutting Temperature compound/30% sucrose in PBS), and then frozen as described previously (69). Cryosections (12 μm thick) were cut with a cryostat-microtome (CM1850, Leica); incubated with primary antibodies: mouse monoclonal 1D4 (1 μg/ml, 1:10 000; anti-rod opsin, from R. Molday, University of British Columbia), mouse monoclonal KPSA1 (anti-RPE65, 1:400, generated in K. Palczewski Laboratory) or biotylated-peanut agglutinin (PNA, for labeling cones, 1:400 from Vector Laboratories); and visualized with goat anti-mouse Alexa Fluor Cy3– or 488–conjugated IgGs (1:500, Jackson ImmunoResearch Laboratories Inc.) for 1D4 and KPSA1, or Alexa Fluor 488-conjugated streptavidin (1:500, Invitrogen) for PNA. Nuclei were counterstained with DAPI. Fluorescence was detected with a confocal microscope (TCS SP5, Leica).

SD-OCT and fundus acquisition

With pupils fully dilated with 1% tropicamide (Falcon Pharmaceuticals, Fort Worth, TX, USA), mice were anesthetized with

an intraperitoneal injection of ketamine (100 mg/kg, Ketaset, Fort Dodge, IA, USA) and xylazine (4 mg/kg, AnaSed, Lloyd Laboratories, Shenandoah, IA, USA). Whiskers were trimmed carefully to avoid image artifacts. OCT images were acquired with linear B-scan mode by employing ultra-high-resolution SD-OCT (Bioptigen).

Mouse fundus imaging was then performed with a cSLO (SpectralisHRA2, Heidelberg Engineering, Heidelberg, Germany) with a 55° lens. The near infrared reflectance image (IR mode, 820 nm laser) was used to align the fundus camera relative to the pupil to obtain an evenly illuminated fundus image. An ICGA mode (790 nm) laser was used for angiography 10 min after mice were injected intraperitoneally with ICG (15 mg/kg, Acros Organics, NJ, USA).

MRI and CT scans

MRI scans were performed with three mice per genotype. All animals were anesthetized with 1–3% isoflurane anesthesia in oxygen gas during the imaging scans. For MRI imaging procedures, high-resolution (117 × 117 μm) coronal and sagittal images were acquired by multiecho spin echo acquisition (TR/TE = 3000 ms/12 ms) on a Bruker Biospec 9.4T MRI scanner (Bruker Biospin, Billerica, MA, USA). Slice thicknesses of 500 and 700 μm were used for coronal and sagittal images, respectively. Mice were scanned with a Siemens Inveon CT scanner to obtain whole animal high-resolution (e.g. 29 μm) 3D anatomic images.

SUPPLEMENTARY MATERIAL

Supplementary Material is available at *HMG* online.

ACKNOWLEDGEMENTS

We thank Victoria Flatt for outstanding technical assistance. The authors are grateful to Dr Leslie T. Webster, Jr (Case Western Reserve University) for critical comments and important suggestions on the manuscript. We are thankful to Dr Loredana Quadro (Rutgers) and Dr William Blaner (Columbia) for the gift of RBP4-deficient mice. We thank Dr Norbert Ghyselinck (IGBMC, Strasbourg, France) for helpful discussion about neomycin resistance cassettes. K.P. is John H. Hord Professor of Pharmacology. We also thank Maryanne Pendergast and the Neurosciences Imaging Center for assistance with confocal imaging.

Conflict of Interest statement. None declared.

FUNDING

This work was supported by US National Institute of Health grants (EY019641, EY020551). K.P. is John H. Hord Professor of Pharmacology.

REFERENCES

1. Shah, S.P., Taylor, A.E., Sowden, J.C., Ragge, N.K., Russell-Eggitt, I., Rahi, J.S. and Gilbert, C.E. (2011) Anophthalmos, microphthalmos, and typical coloboma in the United Kingdom: a prospective study of incidence and risk. *Invest. Ophthalmol. Vis. Sci.*, **52**, 558–564.
2. Slavotinek, A.M. (2011) Eye development genes and known syndromes. *Mol. Genet. Metab.*, **104**, 448–456.
3. Gerth-Kahlert, C., Williamson, K., Ansari, M., Rainger, J.K., Hingst, V., Zimmermann, T., Tech, S., Guthoff, R.F., van Heyningen, V. and Fitzpatrick, D.R. (2013) Clinical and mutation analysis of 51 probands with anophthalmia and/or severe microphthalmia from a single center. *Mol. Genet. Genomic Med.*, **1**, 15–31.
4. Golzio, C., Martinovic-Bouriel, J., Thomas, S., Mougou-Zrelli, S., Grattagliano-Bessieres, B., Bonniere, M., Delahaye, S., Munnich, A., Encha-Razavi, F., Lyonnet, S. *et al.* (2007) Matthew-Wood syndrome is caused by truncating mutations in the retinol-binding protein receptor gene STRA6. *Am. J. Hum. Genet.*, **80**, 1179–1187.
5. Pasutto, F., Sticht, H., Hammersen, G., Gillessen-Kaesbach, G., Fitzpatrick, D.R., Nurnberg, G., Brasch, F., Schirmer-Zimmermann, H., Tolmie, J.L., Chitayat, D. *et al.* (2007) Mutations in STRA6 cause a broad spectrum of malformations including anophthalmia, congenital heart defects, diaphragmatic hernia, alveolar capillary dysplasia, lung hypoplasia, and mental retardation. *Am. J. Hum. Genet.*, **80**, 550–560.
6. Chassaing, N., Golzio, C., Odent, S., Lequeux, L., Vigouroux, A., Martinovic-Bouriel, J., Tiziano, F.D., Masini, L., Piro, F., Maragliano, G. *et al.* (2009) Phenotypic spectrum of STRA6 mutations: from Matthew-Wood syndrome to non-lethal anophthalmia. *Hum. Mutat.*, **30**, E673–E681.
7. Casey, J., Kawaguchi, R., Morrissey, M., Sun, H., McGettigan, P., Nielsen, J.E., Conroy, J., Regan, R., Kenny, E., Cormican, P. *et al.* (2011) First implication of STRA6 mutations in isolated anophthalmia, microphthalmia, and coloboma: a new dimension to the STRA6 phenotype. *Hum. Mutat.*, **32**, 1417–1426.
8. Bouillet, P., Sapin, V., Chazaud, C., Messaddeq, N., Decimo, D., Dolle, P. and Chambon, P. (1997) Developmental expression pattern of Stra6, a retinoic acid-responsive gene encoding a new type of membrane protein. *Mech. Dev.*, **63**, 173–186.
9. Kawaguchi, R., Yu, J., Honda, J., Hu, J., Whitelegge, J., Ping, P., Wiita, P., Bok, D. and Sun, H. (2007) A membrane receptor for retinol binding protein mediates cellular uptake of vitamin A. *Science*, **315**, 820–825.
10. Sun, H. and Kawaguchi, R. (2011) The membrane receptor for plasma retinol-binding protein, a new type of cell-surface receptor. *Int. Rev. Cell Mol. Biol.*, **288**, 1–41.
11. Quadro, L., Blaner, W.S., Salchow, D.J., Vogel, S., Piantedosi, R., Gouras, P., Freeman, S., Cosma, M.P., Colantuoni, V. and Gottesman, M.E. (1999) Impaired retinal function and vitamin A availability in mice lacking retinol-binding protein. *EMBO J.*, **18**, 4633–4644.
12. D'Ambrosio, D.N., Clugston, R.D. and Blaner, W.S. (2011) Vitamin A metabolism: an update. *Nutrients*, **3**, 63–103.
13. Isken, A., Golczak, M., Oberhauser, V., Hunzelmann, S., Driever, W., Imanishi, Y., Palczewski, K. and von Lintig, J. (2008) RBP4 disrupts vitamin A uptake homeostasis in a STRA6-deficient animal model for Matthew-Wood syndrome. *Cell. Metab.*, **7**, 258–268.
14. Kawaguchi, R., Yu, J., Ter-Stepanian, M., Zhong, M., Cheng, G., Yuan, Q., Jin, M., Travis, G.H., Ong, D. and Sun, H. (2011) Receptor-mediated cellular uptake mechanism that couples to intracellular storage. *ACS Chem. Biol.*, **6**, 1041–1045.
15. Kawaguchi, R., Zhong, M., Kassai, M., Ter-Stepanian, M. and Sun, H. (2012) STRA6-catalyzed vitamin A influx, efflux, and exchange. *J. Membrane Biol.*, **245**, 731–745.
16. Amengual, J., Golczak, M., Palczewski, K. and von Lintig, J. (2012) Lecithin:retinol acyltransferase is critical for cellular uptake of vitamin A from serum retinol-binding protein. *J. Biol. Chem.*, **287**, 24216–24227.
17. Rhinn, M. and Dolle, P. (2012) Retinoic acid signalling during development. *Development*, **139**, 843–858.
18. Clagett-Dame, M. and DeLuca, H.F. (2002) The role of vitamin A in mammalian reproduction and embryonic development. *Annu. Rev. Nutr.*, **22**, 347–381.
19. Kawaguchi, R., Yu, J., Wiita, P., Honda, J. and Sun, H. (2008) An essential ligand-binding domain in the membrane receptor for retinol-binding protein revealed by large-scale mutagenesis and a human polymorphism. *J. Biol. Chem.*, **283**, 15160–15168.
20. Ruiz, A., Mark, M., Jacobs, H., Klopfenstein, M., Hu, J., Lloyd, M., Habib, S., Tosha, C., Radu, R.A., Ghyselinck, N.B. *et al.* (2012) Retinoid content, visual responses, and ocular morphology are compromised in the retinas of

mice lacking the retinol-binding protein receptor, STRA6. *Invest. Ophthalmol. Vis. Sci.*, **53**, 3027–3039.
21. Berry, D.C., Jacobs, H., Marwarha, G., Gely-Pernot, A., O'Byrne, S.M., Desantis, D., Klopfenstein, M., Feret, B., Dennefeld, C., Blaner, W.S. *et al.* (2013) The STRA6 receptor is essential for retinol-binding protein-induced insulin resistance but not for maintaining vitamin A homeostasis in tissues other than the eye. *J. Biol. Chem.*, **288**, 24528–24539.
22. Terra, R., Wang, X., Hu, Y., Charpentier, T., Lamarre, A., Zhong, M., Sun, H., Mao, J., Qi, S., Luo, H. *et al.* (2013) To investigate the necessity of STRA6 upregulation in T cells during T cell immune responses. *PLoS ONE*, **8**, e82808.
23. Biesalski, H.K., Frank, J., Beck, S.C., Heinrich, F., Illek, B., Reifen, R., Gollnick, H., Seeliger, M.W., Wissinger, B. and Zrenner, E. (1999) Biochemical but not clinical vitamin A deficiency results from mutations in the gene for retinol binding protein. *Am. J. Clin. Nutr.*, **69**, 931–936.
24. Seeliger, M.W., Biesalski, H.K., Wissinger, B., Gollnick, H., Gielen, S., Frank, J., Beck, S. and Zrenner, E. (1999) Phenotype in retinol deficiency due to a hereditary defect in retinol binding protein synthesis. *Invest. Ophthalmol. Vis. Sci.*, **40**, 3–11.
25. Berry, D.C., Jin, H., Majumdar, A. and Noy, N. (2011) Signaling by vitamin A and retinol-binding protein regulates gene expression to inhibit insulin responses. *Proc. Natl. Acad. Sci. USA*, **108**, 4340–4345.
26. Zemany, L., Kraus, B.J., Norseen, J., Saito, T., Peroni, O.D., Johnson, R.L. and Kahn, B.B. (2014) Downregulation of STRA6 in adipocytes and adipose stromovascular fraction in obesity and effects of adipocyte-specific STRA6 knockdown in vivo. *Mol. Cell Biol.*, **34**, 1170–1186.
27. Muenzner, M., Tuvia, N., Deutschmann, C., Witte, N., Tolkachov, A., Valai, A., Henze, A., Sander, L.E., Raila, J. and Schupp, M. (2013) RBP4 and its membrane receptor STRA6 control adipogenesis by regulating cellular retinoid homeostasis and RARalpha activity. *Mol. Cell Biol.*, **33**, 4068–4082.
28. Graham, T.E., Yang, Q., Bluher, M., Hammarstedt, A., Ciaraldi, T.P., Henry, R.R., Wason, C.J., Oberbach, A., Jansson, P.A., Smith, U. *et al.* (2006) Retinol-binding protein 4 and insulin resistance in lean, obese, and diabetic subjects. *N. Engl. J. Med.*, **354**, 2552–2563.
29. Sun, Q., Kiernan, U.A., Shi, L., Phillips, D.A., Kahn, B.B., Hu, F.B., Manson, J.E., Albert, C.M. and Rexrode, K.M. (2013) Plasma retinol-binding protein 4 (RBP4) levels and risk of coronary heart disease: a prospective analysis among women in the nurses' health study. *Circulation*, **127**, 1938–1947.
30. Lehtinen, M.K., Bjornsson, C.S., Dymecki, S.M., Gilbertson, R.J., Holtzman, D.M. and Monuki, E.S. (2013) The choroid plexus and cerebrospinal fluid: emerging roles in development, disease, and therapy. *J. Neurosci.*, **33**, 17553–17559.
31. Mizee, M.R., Wooldrik, D., Lakeman, K.A., van het Hof, B., Drexhage, J.A., Geerts, D., Bugiani, M., Aronica, E., Mebius, R.E., Prat, A. *et al.* (2013) Retinoic acid induces blood-brain barrier development. *J. Neurosci.*, **33**, 1660–1671.
32. Olson, E.N., Arnold, H.H., Rigby, P.W. and Wold, B.J. (1996) Know your neighbors: three phenotypes in null mutants of the myogenic bHLH gene MRF4. *Cell*, **85**, 1–4.
33. Pham, C.T., MacIvor, D.M., Hug, B.A., Heusel, J.W. and Ley, T.J. (1996) Long-range disruption of gene expression by a selectable marker cassette. *Proc. Natl. Acad. Sci. USA*, **93**, 13090–13095.
34. Palczewski, K. (2010) Retinoids for treatment of retinal diseases. *Trends Pharmacol. Sci.*, **31**, 284–295.
35. Duan, W. and Schreiber, G. (1992) Expression of retinol-binding protein mRNA in mammalian choroid plexus. *Comp. Biochem. Physiol.*, **101**, 399–406.
36. MacDonald, P.N., Bok, D. and Ong, D.E. (1990) Localization of cellular retinol-binding protein and retinol-binding protein in cells comprising the blood-brain barrier of rat and human. *Proc. Natl. Acad. Sci. USA*, **87**, 4265–4269.
37. Golczak, M., Maeda, A., Bereta, G., Maeda, T., Kiser, P.D., Hunzelmann, S., von Lintig, J., Blaner, W.S. and Palczewski, K. (2008) Metabolic basis of visual cycle inhibition by retinoid and nonretinoid compounds in the vertebrate retina. *J. Biol. Chem.*, **283**, 9543–9554.
38. Wu, L. and Ross, A.C. (2011) Acidic retinoids synergize with vitamin A to enhance retinol uptake and STRA6, LRAT, and CYP26B1 expression in neonatal lung. *J. Lipid Res.*, **51**, 378–387.
39. Motani, A., Wang, Z., Conn, M., Siegler, K., Zhang, Y., Liu, Q., Johnstone, S., Xu, H., Thibault, S., Wang, Y. *et al.* (2009) Identification and characterization of a non-retinoid ligand for retinol-binding protein 4 which lowers serum retinol-binding protein 4 levels in vivo. *J. Biol. Chem.*, **284**, 7673–7680.
40. Heller, M. and Bok, D. (1976) A specific receptor for retinol binding protein as detected by the binding of human and bovine retinol binding protein to pigment epithelial cells. *Am. J. Ophthalmol.*, **81**, 93–97.
41. Maraini, G., Ottonello, S., Gozzoli, F. and Merli, A. (1977) Identification of a membrane protein binding the retinol in retinal pigment epithelium. *Nature*, **265**, 68–69.
42. Chazaud, C., Bouillet, P., Oulad-Abdelghani, M. and Dolle, P. (1996) Restricted expression of a novel retinoic acid responsive gene during limb bud dorsoventral patterning and endochondral ossification. *Dev. Genet.*, **19**, 66–73.
43. Lammer, E.J., Chen, D.T., Hoar, R.M., Agnish, N.D., Benke, P.J., Braun, J.T., Curry, C.J., Fernhoff, P.M., Grix, A.W. Jr, Lott, I.T. *et al.* (1985) Retinoic acid embryopathy. *N. Engl. J. Med.*, **313**, 837–841.
44. Goez, H.R., Scott, O. and Hasal, S. (2011) Fetal exposure to alcohol, developmental brain anomaly, and vitamin a deficiency: a case report. *J. Child Neurol.*, **26**, 231–234.
45. Woollam, D.H. and Millen, J.W. (1955) Effect of vitamin A deficiency on the cerebro-spinal fluid pressure of the chick. *Nature*, **175**, 41–42.
46. Millen, J.W. and Dickson, A.D. (1957) The effect of vitamin A upon the cerebrospinal-fluid pressures of young rabbits suffering from hydrocephalus due to maternal hypovitaminosis A. *Br. J. Nutr.*, **11**, 440–446.
47. Matt, N., Dupe, V., Garnier, J.M., Dennefeld, C., Chambon, P., Mark, M. and Ghyselinck, N.B. (2005) Retinoic acid-dependent eye morphogenesis is orchestrated by neural crest cells. *Development*, **132**, 4789–4800.
48. Janssen, J.J., Kuhlmann, E.D., van Vugt, A.H., Winkens, H.J., Janssen, B.P., Deutman, A.F. and Driessen, C.A. (2000) Retinoic acid delays transcription of human retinal pigment neuroepithelium marker genes in ARPE-19 cells. *Neuroreport*, **11**, 1571–1579.
49. Yasunari, T., Yanagihara, N., Komatsu, T., Moriwaki, M., Shiraki, K., Miki, T., Yano, Y. and Otani, S. (1999) Effect of retinoic acid on proliferation and polyamine metabolism in cultured bovine retinal pigment epithelial cells. *Ophthalmic Res.*, **31**, 24–32.
50. Kishi, H., Kuroda, E., Mishima, H.K. and Yamashita, U. (2001) Role of TGF-beta in the retinoic acid-induced inhibition of proliferation and melanin synthesis in chick retinal pigment epithelial cells in vitro. *Cell Biol. Int.*, **25**, 1125–1129.
51. Rong, J. and Liu, S. (2011) Effect of all-trans retinoic acid on the barrier function in human retinal pigment epithelial cells. *Biochem. Biophys. Res. Commun.*, **407**, 605–609.
52. Tombran-Tink, J., Lara, N., Apricio, S.E., Potluri, P., Gee, S., Ma, J.X., Chader, G. and Barnstable, C.J. (2004) Retinoic acid and dexamethasone regulate the expression of PEDF in retinal and endothelial cells. *Exp. Eye Res.*, **78**, 945–955.
53. Uchida, H., Hayashi, H., Kuroki, M., Uno, K., Yamada, H., Yamashita, Y., Tombran-Tink, J. and Oshima, K. (2005) Vitamin A up-regulates the expression of thrombospondin-1 and pigment epithelium-derived factor in retinal pigment epithelial cells. *Exp. Eye Res.*, **80**, 23–30.
54. Redmond, T.M., Yu, S., Lee, E., Bok, D., Hamasaki, D., Chen, N., Goletz, P., Ma, J.X., Crouch, R.K. and Pfeifer, K. (1998) Rpe65 is necessary for production of 11-cis-vitamin A in the retinal visual cycle. *Nat. Genet.*, **20**, 344–351.
55. Rohrer, B., Lohr, H.R., Humphries, P., Redmond, T.M., Seeliger, M.W. and Crouch, R.K. (2005) Cone opsin mislocalization in Rpe65-/- mice: a defect that can be corrected by 11-cis retinal. *Invest. Ophthalmol. Vis. Sci.*, **46**, 3876–3882.
56. Samardzija, M., Tanimoto, N., Kostic, C., Beck, S., Oberhauser, V., Joly, S., Thiersch, M., Fahl, E., Arsenijevic, Y., von Lintig, J. *et al.* (2009) In conditions of limited chromophore supply rods entrap 11-cis-retinal leading to loss of cone function and cell death. *Hum. Mol. Genet.*, **18**, 1266–1275.
57. Batten, M.L., Imanishi, Y., Maeda, T., Tu, D.C., Moise, A.R., Bronson, D., Possin, D., Van Gelder, R.N., Baehr, W. and Palczewski, K. (2004) Lecithin-retinol acyltransferase is essential for accumulation of all-trans-retinyl esters in the eye and in the liver. *J. Biol. Chem.*, **279**, 10422–10432.
58. McIlroy, G.D., Delibegovic, M., Owen, C., Stoney, P.N., Shearer, K.D., McCaffery, P.J. and Mody, N. (2013) Fenretinide treatment prevents diet-induced obesity in association with major alterations in retinoid homeostatic gene expression in adipose, liver, and hypothalamus. *Diabetes*, **62**, 825–836.
59. Alapatt, P., Guo, F., Komanetsky, S.M., Wang, S., Cai, J., Sargsyan, A., Rodriguez Diaz, E., Bacon, B.T., Aryal, P. and Graham, T.E. (2012) Liver

retinol transporter and receptor for serum retinol binding protein (RBP4). *J. Biol. Chem.*, **288**, 1250–1265.
60. Yahyavi, M., Abouzeid, H., Gawdat, G., de Preux, A.S., Xiao, T., Bardakjian, T., Schneider, A., Choi, A., Jorgenson, E., Baier, H. *et al.* (2013) ALDH1A3 loss of function causes bilateral anophthalmia/microphthalmia and hypoplasia of the optic nerve and optic chiasm. *Hum. Mol. Genet.*, **22**, 3250–3258.
61. Molotkov, A., Molotkova, N. and Duester, G. (2006) Retinoic acid guides eye morphogenetic movements via paracrine signaling but is unnecessary for retinal dorsoventral patterning. *Development*, **133**, 1901–1910.
62. Wassef, L. and Quadro, L. (2011) Uptake of dietary retinoids at the maternal-fetal barrier: in vivo evidence for the role of lipoprotein lipase and alternative pathways. *J. Biol. Chem.*, **286**, 32198–32207.
63. Quadro, L., Hamberger, L., Gottesman, M.E., Wang, F., Colantuoni, V., Blaner, W.S. and Mendelsohn, C.L. (2005) Pathways of vitamin A delivery to the embryo: insights from a new tunable model of embryonic vitamin A deficiency. *Endocrinology*, **146**, 4479–4490.
64. Redondo, C., Vouropoulou, M., Evans, J. and Findlay, J.B. (2008) Identification of the retinol-binding protein (RBP) interaction site and functional state of RBPs for the membrane receptor. *FASEB J.*, **22**, 1043–1054.
65. Sundaram, M., Sivaprasadarao, A., DeSousa, M.M. and Findlay, J.B. (1998) The transfer of retinol from serum retinol-binding protein to cellular retinol-binding protein is mediated by a membrane receptor. *J. Biol. Chem.*, **273**, 3336–3342.
66. Kim, Y.K., Wassef, L., Hamberger, L., Piantedosi, R., Palczewski, K., Blaner, W.S. and Quadro, L. (2008) Retinyl ester formation by lecithin: retinol acyltransferase is a key regulator of retinoid homeostasis in mouse embryogenesis. *J. Biol. Chem.*, **283**, 5611–5621.
67. Kim, T.S., Maeda, A., Maeda, T., Heinlein, C., Kedishvili, N., Palczewski, K. and Nelson, P.S. (2005) Delayed dark adaptation in 11-cis-retinol dehydrogenase-deficient mice: a role of RDH11 in visual processes in vivo. *J. Biol. Chem.*, **280**, 8694–8704.
68. Amengual, J., Golczak, M., Palczewski, K. and von Lintig, J. (2012) Lecithin:retinol acyltransferase is critical for cellular uptake of vitamin A from serum retinol-binding protein. *J. Biol. Chem.*, **287**, 24216–24227.
69. Zhang, N., Kolesnikov, A.V., Jastrzebska, B., Mustafi, D., Sawada, O., Maeda, T., Genoud, C., Engel, A., Kefalov, V.J. and Palczewski, K. (2013) Autosomal recessive retinitis pigmentosa E150 K opsin mice exhibit photoreceptor disorganization. *J. Clin. Invest.*, **123**, 121–137.